

SADI: A SELF-ADAPTIVE DECOMPOSED INTERPRETABLE FRAMEWORK FOR ELECTRIC LOAD FORECASTING UNDER EXTREME EVENTS

Hengbo Liu^{1†}

Ziqing Ma^{1†}
Yi Wang³

Linxiao Yang¹
Qingsong Wen²

Tian Zhou¹
Liang Sun^{2*}

Rui Xia¹

¹ DAMO Academy, Alibaba Group, Hangzhou, China

² DAMO Academy, Alibaba Group, Bellevue, US

³ The University of Hong Kong, Hong Kong, China

ABSTRACT

Accurate prediction of electric load is crucial in power grid planning and management. In this paper, we solve the electric load forecasting problem under extreme events such as scorching heats. One challenge for accurate forecasting is the lack of training samples under extreme conditions. Also load usually changes dramatically in these extreme conditions, which calls for interpretable model to make better decisions. In this paper, we propose a novel forecasting framework, named Self-adaptive Decomposed Interpretable framework (SaDI), which ensembles long-term trend, short-term trend, and period modelings to capture temporal characteristics in different components. The external variable triggered loss is proposed for the imbalanced learning under extreme events. Furthermore, Generalized Additive Model (GAM) is employed in the framework for desirable interpretability. The experiments on both Central China electric load and public energy meters from buildings show that the proposed SaDI framework achieves average 22.14% improvement compared with the current state-of-the-art algorithms in forecasting under extreme events in terms of daily mean of normalized RMSE. Code, Public datasets, and Appendix are available at: <https://doi.org/10.24433/CO.9696980.v1>.

Index Terms— Time series forecasting, electric load forecasting, extreme events, XAI

1. INTRODUCTION

The electric load forecasting (ELF) is one of the major problems facing the power industry [1, 2]. Especially, when extreme events occur, load always fluctuates and threatens the electric grid. For example, China issued the highest heat alert for almost 70 cities in July 2022, and the electric load increased dramatically due to the extensive use of air conditioner. Thus, accurate forecasting under extreme events is highly desirable. Despite its importance, forecasting under extreme events is not well investigated. Modern deep

learning based methods for time series forecasting [3, 4, 5] often focus on minimizing the global loss, which ignore data skew between normal cases and extreme events and fail to achieve desirable performance under extreme events. Note that forecasting under extreme events is closely related to regression problems on imbalanced data, for which numerous methods have been proposed, such as SMOTER [6], SMOGN [7], reweighting [8], transfer learning [9], label distribution smooth (LDS) [10], etc. More related work can be found in Appendix B.

To deal with load forecasting under extreme events, especially complicated load series mixed with long-term trend, short-term trend, and periodical patterns, we propose a novel framework named Self-adaptive Decomposed Interpretable framework (SaDI). It decomposes the original load series into three components, which are modeled differently. We observe that the effects of extreme events caused by external covariables dominate load patterns. For example, the excessively high load in July 2022 in China is mainly caused by the high temperature. Thus, we further design an External Triggered Loss (ETL) to improve the forecasting performance. In addition, interpretability is also an important factor for system operators [11]. We employ Generalized Additive Models (GAM) [12, 13] to learn the explainable relationship between the short-term trend and input features, where GAM is a class of intrinsic explainable methods that formulate the predicate function as a summation of functions that only rely on single features [14]. To summarize, our contributions are listed as follows:

1. The proposed SaDI is robust to extreme events thanks to its decomposed structure, and the decomposed series are treated with different strategies.
2. The proposed SaDI is interpretable by adopting a Generalized Additive Model (GAM) for modeling the relationship between the target and input features.
3. We introduce a loss triggered by external variables (ETL), which further enhances the model with robust performance under extreme events.

[†] Equal contribution

* Corresponding authors

2. STATEMENT OF THE PROBLEM

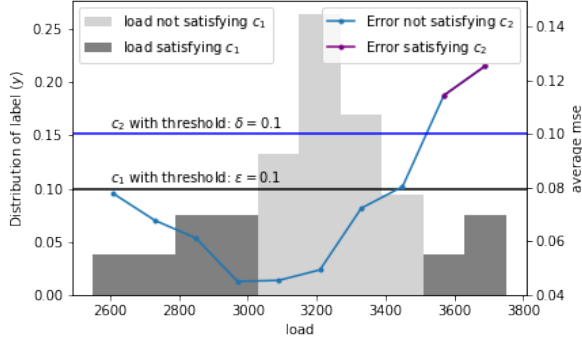


Fig. 1: Illustration of how to define an *Extreme Event* with two conditions c_1 & c_2 . c_1 : the probability of the label is lower than a threshold ϵ . c_2 : the forecasting error is higher than a threshold δ .

Extreme events are rare and random, but play a critical role in many real applications. In most cases, extreme events can be reflected by one or several indicators, either the label or the features. In this paper, the dataset with a size of N is represented as: $D = \{d_1, \dots, d_i, \dots, d_N\}$, where $d_i = (\mathbf{x}_i, y_i)$, \mathbf{x}_i is the input features of i^{th} sample, y_i is the label. Then the subset of samples under extreme events D_{ex} can be obtained by:

$$D_{ex} = \{d_i | c(\mathbf{x}_i, y_i), d_i \in D\}, \quad (1)$$

where $c(\cdot)$ is extreme events condition. For the construction of c , we assume that the extreme event happens when the label is rare, and at the same time, the prediction error is high. So we have $c = c_1 \cap c_2$, and:

$$c_1 : P(b_j) < \epsilon$$

$$c_2 : \sum_{(\mathbf{x}_i, y_i) \in b_j} \|f(\mathbf{x}_i) - y_i\|_p > \delta$$

Here, we separate the dataset $D = \{(\mathbf{x}_i, y_i)\}$ into bins $\{b_j\}$. c_1 means that the probability of the labels $\{y_i\}$ in bin b_j is less than ϵ , which indicates the rareness of the extreme event. c_2 means that the prediction error (p-norm) in b_j is more than δ . $f(\cdot)$ is a baseline forecasting model, e.g., LightGBM or other deep learning methods. An illustration is depicted in Figure 1.

3. METHODOLOGY

3.1. Overall Framework

The overall framework of our proposed model, SaDI, is an ensemble structure as shown in Figure 2. The input series is first processed by decomposition modules. Then we use Linear regression to model long-term trend, GAM with external

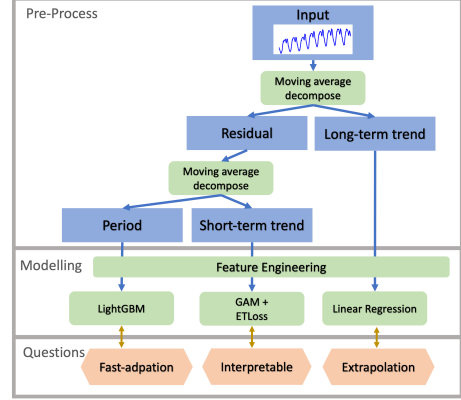


Fig. 2: The overall framework of SaDI, which consists of decomposition-based pre-processing, feature engineering, and three models to deal with different decomposed components, respectively.

variable triggered loss to model short-term trend, and LightGBM to model period.

3.2. Decomposition-based Modeling

The electric load series are often a mixture of trends and periods. We decompose the electric power load (y_t) into a long-term trend (y_t^{LT}), a short-term trend (y_t^{ST}), and a periodic component (y_t^S) as: $y_t = y_t^{LT} + y_t^{ST} + y_t^S$. We adopt a moving-average-based decomposition method defined as:

$$y_t^{LT} = MovAvg(y_t), R = y_t - y_t^{LT}, \quad (2)$$

$$y_t^{ST} = MovAvg(R), y_t^S = R - y_t^{ST}. \quad (3)$$

The decomposed components are illustrated in Figure 3 (Mid). Three sub-series estimations are discussed below.

Long-term Trend Modeling The long-term trend, also known as the yearly trend, is a smooth and continuously growing curve as shown in Figure 3 (Mid). The tendency of electric load series strongly correlates to the growth of district GDP or climate change, such as global warming [15]. We use linear regression which is capable of handling the simple pattern of long-term trend while maintaining the ability of extrapolation on rising tendency.

Short-term Trend Modeling After removing the long-term trend, the residual combines periodical-term and short-term trend. In short-term trend, due to the rareness of extremely hot weather in training data, a sudden increase in load would be difficult for the model to capture. To solve this, we introduce an external variable triggered loss (ETL) which will be discussed in Section 3.3. We leverage GAM as a backbone model in Section 3.4 for interpretability with ETL.

Period Modeling After removing the long-term trend and the short-term trend, We use LightGBM to model the periodic daily pattern without long-term and short-term trend.

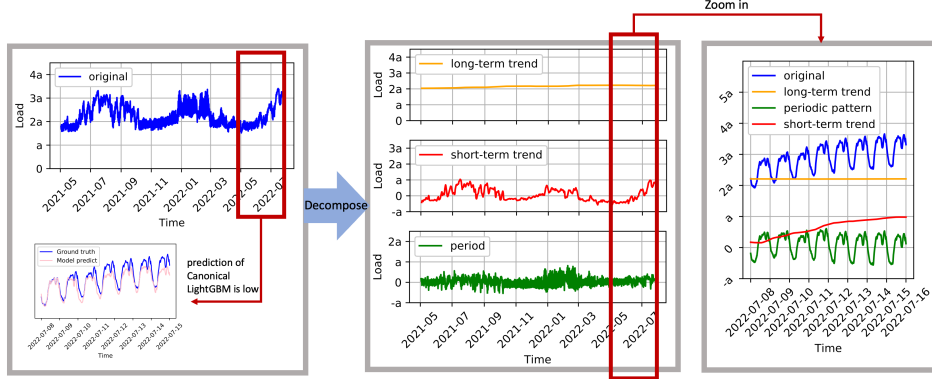


Fig. 3: Decomposition of electric load series. (Left up): The original series. (Left down) The prediction given by canonical LightGBM is low under extreme events. (Mid): Decomposition of original load into three components: long-term trend, short-term trend, and period. (Right): zoom in on the three components. The Y axis is masked for confidentiality purposes.

3.3. External-variable Triggered Loss

In our framework, after decomposition, the short-term trend is affected by external variables like weather indicators. To quantitatively characterize the effects of the external variables, an External-variable Triggered Loss (ETL) function is designed as:

$$ETL = \sum_{t=1}^N \left[S \left(\sum_{q=1}^Q \lambda_q x_{t,q}^e \right) * (\hat{y}_t - y_t^{ST})^2 \right], \quad (4)$$

where x^e denotes the external variable, N denotes the number of samples, λ_q denotes the user-defined weight for the q^{th} external features x_q^e (for example, in load forecasting, we give large weights for temperature), and \hat{y}_t denotes the output of GAM. $S(\cdot)$ is a non-linear score function, which gives different weight to each sample according to its extreme level.

We now discuss the selection of weights $\{\lambda_q\}$ and score function $S(\cdot)$. we set a different weight to selected external variables by correlation analysis when extreme value occurs. Specifically, when scorching heats happened, temperature is selected as an external variable as a result of high correlation coefficient with target load. It can also be explained physically that residential usage of air conditioning load would increase significantly when air temperature increases. In this simple case, temperature is the only external variable. Let $X_{t,1}^e$ denote the feature that represents temperature, we set $\lambda_1 = 1$ and $\lambda_j = 0, \forall j \neq 1$. To emphasize the weight of samples with extremely high temperatures, we set $S(\cdot)$ as

$$S(T_t) = \begin{cases} \frac{2}{1+e^{-(T_t-K)}} & T_t > K, \\ 1 & T_t \leq K, \end{cases} \quad (5)$$

where $T_t = \lambda_1 X_{t,1}^e$, $S(\cdot)$ is a piece-wise function adopted to give heavier weights to samples with temperatures higher than K , and K is set as a predefined threshold value for different tasks. Multi external variables ETL expression can be easily expanded with 4.

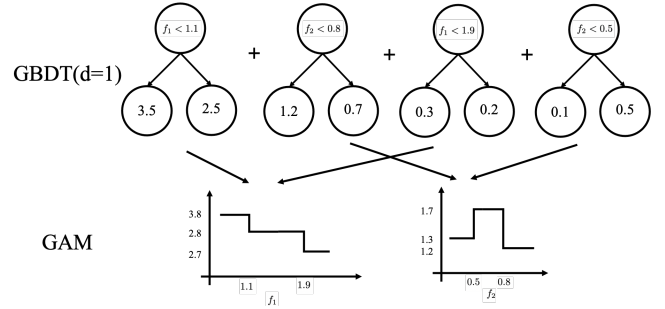


Fig. 4: Example of converting GBDT to GAM.

3.4. Generalized Additive Model (GAM)

As discussed above, the short-term trend is correlated to external factors. We leverage a GAM model to fit the short-term trend with ETL as loss function, where the short-term trend is formalized as a summation of univariate functions of the external factors. Specifically,

$$y_t^{ST} = \phi_0 + \sum_{q=1}^Q \phi_q(x_{t,q}^e) + \xi_t, \quad (6)$$

where $\phi_q(\cdot)$ denotes the function of the q^{th} external variable, and ξ_t denotes the fitting error. GAM has great interpretability. Given a sample (\mathbf{x}_t, y_t) , we can readily get the contribution of each factor x_t^e as $\phi_q(x_t^e)$. Obviously, the set of $\{\phi_q\}$ that satisfies (6) is not unique. Some works select $\{\phi_q\}$ from the space formed by some particular basis (such as B-spline basis) [16, 17]. Here we implement GAM using GBDT (Gradient Boosting Decision Tree) by setting the depth of trees in GBDT to 1 as shown in Figure 4, which means each tree in only uses one feature, thus no feature interaction is involved.

4. EXPERIMENTS

4.1. Datasets and Baselines

Two electric load datasets are introduced to evaluate our proposed framework. The private datasets are real-world load

Table 1: Performance comparison of load forecasting on two real-world datasets. The best performance is highlighted in bold. Lower values of $nRMSE_d$ and $MAPE_d$ indicate better performance.

| Methods | | Proposed SaDI | | LightGBM | | N-BEATS | | TCN | | LSTM | | LDS* | | EVL | |
|----------|---------|---------------|--------------|--------------|----------|-----------|----------|-----------|----------|-----------|----------|-----------|----------|-----------|----------|
| Datasets | | $nRMSE_d$ | $MAPE_d$ | $nRMSE_d$ | $MAPE_d$ | $nRMSE_d$ | $MAPE_d$ | $nRMSE_d$ | $MAPE_d$ | $nRMSE_d$ | $MAPE_d$ | $nRMSE_d$ | $MAPE_d$ | $nRMSE_d$ | $MAPE_d$ |
| Huazhong | Hubei | 0.052 | 0.045 | 0.066 | 0.058 | 0.106 | 0.099 | 0.075 | 0.067 | 0.112 | 0.114 | 0.061 | 0.054 | 0.064 | 0.054 |
| | Hunan | 0.046 | 0.039 | 0.044 | 0.047 | 0.123 | 0.118 | 0.068 | 0.061 | 0.133 | 0.121 | 0.054 | 0.047 | 0.055 | 0.047 |
| | Henan | 0.059 | 0.051 | 0.082 | 0.072 | 0.105 | 0.097 | 0.099 | 0.090 | 0.128 | 0.114 | 0.079 | 0.069 | 0.080 | 0.069 |
| | Jiangxi | 0.044 | 0.038 | 0.053 | 0.045 | 0.071 | 0.064 | 0.078 | 0.060 | 0.088 | 0.080 | 0.057 | 0.051 | 0.057 | 0.048 |
| Public | Peacock | 0.025 | 0.021 | 0.058 | 0.046 | 0.060 | 0.049 | 0.041 | 0.034 | 0.053 | 0.048 | 0.032 | 0.028 | 0.040 | 0.033 |
| | Rat | 0.086 | 0.077 | 0.163 | 0.152 | 0.174 | 0.157 | 0.130 | 0.121 | 0.194 | 0.183 | 0.130 | 0.121 | 0.156 | 0.147 |
| | Robin | 0.068 | 0.060 | 0.115 | 0.101 | 0.080 | 0.071 | 0.075 | 0.067 | 0.198 | 0.190 | 0.077 | 0.071 | 0.073 | 0.065 |

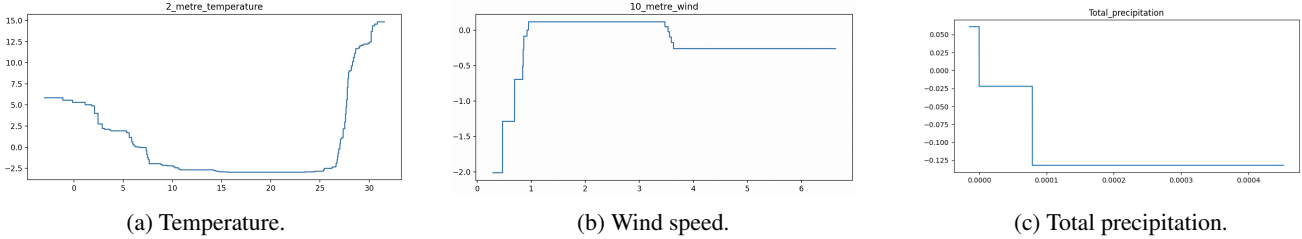


Fig. 5: Learnt functions for temperature, wind speed, and whether special holiday by SaDI.

data from Mid-centre China. The public datasets are from the ASHRAE Great Energy Predictor III competition [18], like Peacock, Rat, and Robin. We compare the performance of SaDI and baselines including LightGBM [19], LSTM [20], N-BEATS [5], TCN [21], EVT [22], LDS [10]. More details about the datasets, baselines, and feature engineering can be found in Appendix C.1, Appendix C.2, and Appendix D, respectively.

4.2. Evaluation Metrics

The most widely used metrics in forecasting are RMSE and MAPE. The RMSE is scale-dependent and unsuitable for comparing forecasting results at different aggregation levels. We adopt the daily mean of normalized root mean squared error $nRMSE_d$ and $MAPE_d$. Their definitions are $nRMSE_d = \frac{1}{N} \sum_{n=1}^N \left(\sqrt{\frac{1}{M} \sum_{i=1}^M \left(\frac{y_i - \hat{y}_i}{y_i} \right)^2} \right)$ and $MAPE_d = \frac{1}{N} \sum_{n=1}^N \left(\frac{1}{M} \sum_{i=1}^M \frac{|y_i - \hat{y}_i|}{y_i} \right)$, where M is the number of points in one day (normally $M=96$, i.e. the sampling interval is 15 minutes), and N is the number of days to be evaluated.

4.3. Performance Comparisons

The results of the baselines and the proposed SaDI are summarized in Table 1. The baselines can be categorized as tree-based models (LightGBM) and deep learning models (N-BEATS, TCN, and LSTM). SaDI, LightGBM, EVL, and LDS share the same feature engineering process. It is observed that SaDI achieves the best results in terms of two metrics on almost all datasets. Specifically, SaDI improves the $nRMSE_d$ and $MAPE_d$ metrics on average by 20.0% and 22.14%, respectively, compared with the best baseline (LDS). Furthermore, Figure 6 shows performance of SaDI on bins of loads compared with the baselines mentioned above. In extreme events when loads exceed 3600 or are below 2800, the RMSE of SaDI is lower than other baselines.

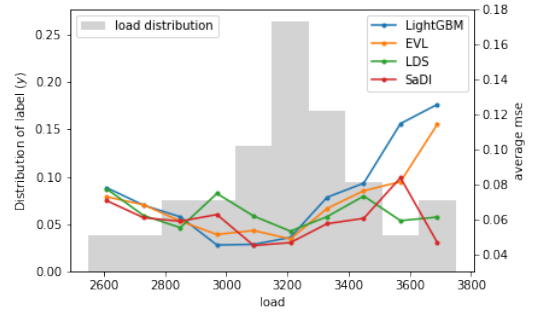


Fig. 6: Performance comparison of SaDI with baselines under the different bins of loads.

4.4. Interpretability

As GAM is employed as a part of SaDI, we can exploit the inherent property of GAM to explain the forecasting of SaDI. As an illustration, the effect on load as functions of temperature, wind speed, and total precipitation by SaDI are plotted in Figure 5. For example, Figure 5a shows how each value of temperature contributes differently to the overall energy load. When the temperature exceeds 26 or is below 7.5 Celsius degree, the energy load changes dramatically.

4.5. Other Experiments

For more experiments (visualization of curves, ablation study, evaluation of speed), please refer to Appendix F.

5. CONCLUSIONS

In this paper, we propose a Self-adaptive Decomposed Interpretable (SaDI) framework for electric load forecasting under extreme events. Our framework decomposes load into long-term, short-term, and period patterns, and deals with them separately with corresponding models. To improve sensitivity to external variables under extreme events, an external variable triggered Loss is designed to guide forecasting models. Furthermore, To explain the forecasting results, generalized additive models are incorporated to provide each feature's contribution to the predicted values quantitatively.

6. REFERENCES

- [1] Shing-Chow Chan, Kai Man Tsui, HC Wu, Yunhe Hou, Yik-Chung Wu, and Felix F Wu, “Load/price forecasting and managing demand response for smart grids: Methodologies and challenges,” *IEEE signal processing magazine*, vol. 29, no. 5, pp. 68–85, 2012.
- [2] Yihong Zhou, Zhaohao Ding, Qingsong Wen, and Yi Wang, “Robust load forecasting towards adversarial attacks via bayesian learning,” *IEEE Transactions on Power Systems*, 2022.
- [3] Tian Zhou, Ziqing Ma, Qingsong Wen, Xue Wang, Liang Sun, and Rong Jin, “FEDformer: Frequency enhanced decomposed transformer for long-term series forecasting,” in *ICML*, 2022.
- [4] Weiqi Chen, Wenwei Wang, Bingqing Peng, Qingsong Wen, Tian Zhou, and Liang Sun, “Learning to rotate: Quaternion transformer for complicated periodical time series forecasting,” in *KDD*, 2022.
- [5] Boris N Oreshkin, Dmitri Carpov, Nicolas Chapados, and Yoshua Bengio, “N-BEATS: Neural basis expansion analysis for interpretable time series forecasting,” in *ICLR*, 2019.
- [6] Luís Torgo, Rita P. Ribeiro, Bernhard Pfahringer, and Paula Branco, “SMOTE for regression,” in *Progress in Artificial Intelligence*, 2013, pp. 378–389.
- [7] Paula Branco, Luís Torgo, and Rita P Ribeiro, “SMOEN: a pre-processing approach for imbalanced regression,” in *Workshop on learning with imbalanced domains: Theory and applications*, 2017, pp. 36–50.
- [8] Michael Steininger, Konstantin Kobs, Pádraig Davidson, Anna Krause, and Andreas Hotho, “Density-based weighting for imbalanced regression,” *Mach. Learn.*, vol. 110, no. 8, pp. 2187–2211, aug 2021.
- [9] Liang Ge, Jing Gao, Hung Ngo, Kang Li, and Aidong Zhang, “On handling negative transfer and imbalanced distributions in multiple source transfer learning,” *Stat. Anal. Data Min.*, vol. 7, no. 4, pp. 254–271, aug 2014.
- [10] Yuzhe Yang, Kaiwen Zha, Yingcong Chen, Hao Wang, and Dina Katabi, “Delving into deep imbalanced regression,” in *ICML*, 2021, pp. 11842–11851.
- [11] Josh Tenenbaum, “Building machines that learn and think like people,” in *Int. Conf. on Autonomous Agents and MultiAgent Systems (AAMAS)*, 2018.
- [12] Yin Lou, Rich Caruana, and Johannes Gehrke, “Intelligible models for classification and regression,” in *KDD*, 2012, pp. 150–158.
- [13] Trevor Hastie and Robert Tibshirani, “Generalized additive models,” *Statistical Science*, vol. 1, no. 3, pp. 297–318, 1986.
- [14] Chun-Hao Chang, Sarah Tan, Benjamin J. Lengerich, Anna Goldenberg, and Rich Caruana, “How interpretable and trustworthy are gams?,” in *KDD ’21: The 27th ACM SIGKDD Conference on Knowledge Discovery and Data Mining, Virtual Event, Singapore, August 14-18, 2021*, Feida Zhu, Beng Chin Ooi, and Chunyan Miao, Eds. 2021, pp. 95–105, ACM.
- [15] Hesham K Alfares and Mohammad Nazeeruddin, “Electric load forecasting: literature survey and classification of methods,” *International journal of systems science*, vol. 33, no. 1, pp. 23–34, 2002.
- [16] Trevor J Hastie, “Generalized additive models,” in *Statistical models in S*, pp. 249–307. Routledge, 2017.
- [17] Amandine Pierrot and Yannig Goude, “Short-term electricity load forecasting with generalized additive models,” *Proceedings of ISAP power*, 2011.
- [18] Clayton Miller, Pandarasamy Arjunan, Anjukan Kathirgamanathan, Chun Fu, et al., “The ASHRAE great energy predictor III competition: Overview and results,” *Science and Technology for the Built Environment*, vol. 26, no. 10, pp. 1427–1447, 2020.
- [19] Guolin Ke, Qi Meng, Thomas Finley, Taifeng Wang, Wei Chen, Weidong Ma, Qiwei Ye, and Tie-Yan Liu, “LightGBM: A highly efficient gradient boosting decision tree,” *NeurIPS*, pp. 3146–3154, 2017.
- [20] Sepp Hochreiter and Jürgen Schmidhuber, “Long Short-Term Memory,” *Neural Computation*, vol. 9, no. 8, pp. 1735–1780, Nov. 1997.
- [21] José F. Torres, M. J. Jiménez-Navarro, Francisco Martínez-Álvarez, and Alicia Troncoso, “Electricity consumption time series forecasting using temporal convolutional networks,” in *Conference of the Spanish Association for Artificial Intelligence (CAEPIA)*, 2021.
- [22] Daizong Ding, Mi Zhang, Xudong Pan, Min Yang, and Xiangnan He, “Modeling extreme events in time series prediction,” in *KDD*, 2019, p. 1114–1122.
- [23] James W Taylor, “Triple seasonal methods for short-term electricity demand forecasting,” *European Journal of Operational Research*, vol. 204, no. 1, pp. 139–152, 2010.
- [24] Rita P. Ribeiro and Nuno Moniz, “Imbalanced regression and extreme value prediction,” *Mach. Learn.*, vol. 109, no. 9–10, pp. 1803–1835, sep 2020.

A. SUPPLEMENTARY MATERIAL INTRODUCTION

The appendices are all in "supplementary_materials" folder. In "Code" Folder, "SaDI_demo.ipynb"(red in Figure 7) is the main entrance function of SaDI framework. sub-folder "ETL.py" (green in Figure 7) gives the definition referred at section "External-variable Triggered Loss" in main paper. "GAM.ipynb" (orange in Figure 7) in "GAM" folder provides source code to generate visible explainable figures. In "Technical" Folder, this "Technical_appendix.pdf" describes appendix materials and illustrates the "Experiments" procedure in the main paper.

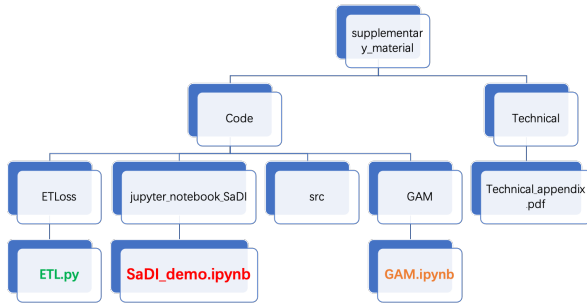


Fig. 7: material introduction

B. RELATED WORK

B.1. Time Series Methods

Numerous research works have been involved in load forecasting in recent years. For cases without extreme events, the forecasting technology both in research [5] and industry [21] is mature. The traditional machine learning methods have limitations in representation power. While, Neural Networks (NN), although being widely investigated in time series tasks, are time-consuming and not suitable for mass deployment. We summarize the challenges and limitations of general time series models in Table 2.

Table 2: Analysis of challenges. LR: linear regression models. Tree: tree-based boosting models. NN: neural networks. SaDI: our method. "+" means the model is capable of handling the challenge. "-" means incapable. "++" means the capacity is prominent.

| Challenge | LR | Tree | NN | SaDI |
|----------------------|----|------|----|------|
| Interpretable | ++ | + | - | ++ |
| Extrapolation | + | - | - | + |
| Fast-adaptation | - | - | - | + |
| Representation power | + | ++ | ++ | ++ |
| Require CPU only | ++ | + | - | + |

B.2. Statistic Methods

Some recent studies in statistics have shown their superiority in dealing with extreme events. Exponential smoothing [23] is widely used in forecasting since it is capable of capturing trend and seasonal characteristics. However, its performance degrades when the forecast horizon increases or some change points information is not perceived. Recently, Extreme Value Loss (EVL) [22] uses Extreme Value Theory (EVT) to detect the possible future occurrences of extreme events. However, EVL is designed based on the assumption that samples are independent and identically distributed (i.i.d), which is seldom satisfied for time series data. Empirical results have shown that the EVL-based method works ordinarily.

B.3. Imbalanced Regression Methods

Work of [24] presents a new approach to dealing with extreme events from the perspective of imbalanced regression (IR), where the objective is to predict extreme values via relevance functions with more attention paid to extreme events through reweighting. Deep Imbalanced Regression combines IR and deep learning to learn continuous targets from naturally imbalanced data. In this model [10], kernel methods are used to smooth label, and feature distributions are learned. However, the skew in distributions of label and features are solved independently, where no explicit relationship is made between the features and the label under extreme events.

C. EXPERIMENT DETAILS

C.1. Datasets

Two Data sets are provided to verify our framework works well. The First data set is private from practical load data from Mid-centre China and South-East China. The Second data is public from the ASHRAE Great Energy Predictor III competition.

First, we use a large-scale private ELF datasets: Huazhong (HZ). HZ dataset contains four sub-datasets for four districts (Hubei, Hunan, Henan, and Jiangxi) in Central China. For each district, the sub-dataset contains one series of electric load and 14 covariates, indicating weather conditions in the future. All time series are sampled with an interval of 15-minutes. Other details of the data set can be found in Table 3.

Secondly, public data set "The Building Data Genome 2"(BDG2) is an open data set made up of 3,053 energy meters from 1,636 buildings. The time range of the times-series data is the two full years and the frequency is hourly measurements of electricity, heating and cooling water, steam, and irrigation meters. These meters were collected from 19 sites across North America and Europe, with one or more meters per building measuring whole building electrical, heating and cooling water. After grouping by 19 sites, related weather

data and cleaned load data are provided for energy forecasting. Other details of the data set can be found in Table 3.

Table 3: Summary of datasets.

| Dataset | | #Features | #Samples | Sample rate |
|----------|---------|-----------|----------|-------------|
| Huazhong | Hubei | 14 | 86113 | 15 min |
| | Hunan | 14 | 86113 | 15 min |
| | Henan | 14 | 86113 | 15 min |
| | Jiangxi | 14 | 86113 | 15 min |
| Public | Peacock | 9 | 70173 | 15 min |
| | Rat | 9 | 70173 | 15 min |
| | Robin | 9 | 70173 | 15 min |

C.1.1. Data Confidential Statements

Raw load data produced by Central-China and South-east China’s grid company is confidential constraint by agreements. Regretly, we could not provided related data in public. The Y axis is masked for confidentiality purposes in both main paper and appendix. However, the Experiments procedure will illustrate here in details to help reader to understand our works.

C.2. Baselines

We compare the performance of SaDI with 6 baselines, including four general time series models and two models specifically designed for extreme events.

1. LightGBM [19]: A tree-based boosting model, feature engineering required.
2. LSTM [20]: Variants of recurrent neural networks, capable of capturing long-term dependency.
3. TCN [21]: Temporal convolutional network, convolution-based time series model.
4. N-BEATS [5]: Fully connected structure with backward and forward residual links, a strong SOTA.
5. EVL [22]: Extreme value loss, which is proposed from EVT, provides better predictions of extreme events.
6. LDS [10]: Deep imbalanced regression model learned from extremely imbalanced data with continuous targets, calibrating target distribution with label distribution smoothing (LDS).

Note that we simplify EVL referred in [22] as only extremely high values events. With the following formulation, u represents the extreme degrees of load,

$$u = \begin{cases} \frac{\hat{y} - \epsilon}{\hat{y}} & \hat{y} > \epsilon \\ 0 & \hat{y} \leq \epsilon \end{cases} \quad (7)$$

where $\epsilon = \mu + K\sigma$ gives the upper bound, with μ, σ being the mean and standard deviation of load. Then, $EVL(\cdot)$ designed in [22] is used in $L_1 = \sum_{t=1}^T \|\hat{y}_t - y_t\| + \lambda_1 EVL(u)$. The gradient and hessian of L_1 can be easily obtained, and subsequently guide tree-base models, such as XGB, LightGBM, with customized loss.

D. FEATURE ENGINEERING

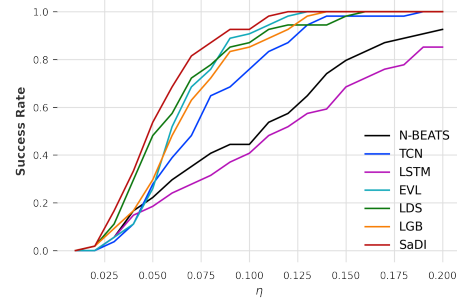


Fig. 8: Success rate with different threshold η of SaDI and baselines on dataset of Hubei (55 days).

Original numerical weather prediction (NWP) factors and history load are main attributes before engineering. It includes 14 NWP attributes, such as ”2 metre temperature”, ” surface pressure”, ”total cloud cover”, ”total precipitation”, ”skin temperature”, etc. History load in time series every 15min is also provided for engineering.

After feature Engineering described in ”SaDI.demo.ipynb”, show in Table 4 below, four categories features: Temporal features, NWP features, Load rolling features, Difference features, Rolling features, totally 63 are generated. For load rolling features, $load_win_i_offset_j_agg$ means rolling $15j$ minutes before with window size i under aggregation method agg , such as $mean, max, min, skew, etc.$ For Difference features, $attribute_diff_offset_j$ means making NWP $attribute$ difference operator with $15j$ minutes before.

E. PSEUDOCODE

We summarize our self-adaptive, decomposed, and interpretable framework for electricity load forecasting under extreme events (referred to as SaDI) in Algorithm 1.

The algorithm mentioned is according to ”SaDI.demo.ipynb” codes enable to help understand our ”SaDI” framework.

DateTimeFeaturizer is used for constructing temporal features with timestamps, such as year, month, day. And some extra-features, such as is workday or not, also can derive from calendar’s information.

DifferenceFeaturizer is used for loading difference weather features ,such as ”2 meter temperature”, ”Surface

Table 4: Features after feature engineering

| Temporal features | NWP features | Load_Rolling features | Difference features |
|-------------------|---------------------|------------------------------|-------------------------------------|
| year | 2_metre_temperature | load_win_7_offset_192_median | 2_metre_temperature_diff_offset_192 |
| month | Surface_pressure | load_win_7_offset_192_mean | Surface_pressure_diff_offset_192 |
| day | Total_cloud_cover | load_win_7_offset_192_min | Total_cloud_cover_diff_offset_192 |
| is_workday | Total_precipitation | load_win_7_offset_192_max | Total_precipitation_diff_offset_192 |
| is_holiday | Skin_temperature | load_win_7_offset_192_std | Skin_temperature_diff_offset_192 |
| is_weekend | ... | load_win_7_offset_192_skew | ... |
| day_of_month_sin | ... | load_win_7_offset_192_q025 | ... |
| ... | ... | ... | ... |

Algorithm 1: SaDI

Input : $\{\mathbf{x}_t, y_t\}_{t=0}^{N-1}$: A set of training samples.
 $\{\mathbf{x}_t\}_{t=N}^{N+m-1}$: features to predict.
Output: Prediction $\{y_t\}_{t=N}^{N+m-1}$.

```

/* Performing decomposition */
1  $y_t^{LT} \leftarrow$  moving average of  $y_t$ 
2  $y_t^{ST} \leftarrow$  moving average of  $y_t - y_t^{LT}$ 
3  $y_t^S \leftarrow y_t - y_t^{LT} - y_t^{ST}$ 
/* Modeling  $y_t^{LT}$  linear model */
4  $\mathbf{w}^* \leftarrow \arg \min \sum_{t=0}^N (y_t^{LT} - \mathbf{w}^T \mathbf{x}_t)^2$ 
/* Learn  $y_t^{ST}$  with GAM */
5 Model1  $\leftarrow$  GAM( training set =  $\{\mathbf{x}_t, y_t^{ST}\}$ ,
loss=ETL)
/* Modeling  $y_t^S$  with lightGBM */
6 Model2  $\leftarrow$  lightgbm( training set =  $\{\mathbf{x}_t, y_t^S\}$ ,
loss=RMSE)
/* Predict using learnt models */
7  $\hat{y}_t^{LT} \leftarrow (\mathbf{w}^*)^T \mathbf{x}_t \quad \forall t = N \dots N + m - 1$ 
8  $\hat{y}_t^{ST} \leftarrow$  Model1( $\mathbf{x}_t$ )  $\quad \forall t = N \dots N + m - 1$ 
9  $\hat{y}_t^S \leftarrow$  Model2( $\mathbf{x}_t$ )  $\quad \forall t = N \dots N + m - 1$ 
10  $y_t \leftarrow \hat{y}_t^{LT} + \hat{y}_t^{ST} + \hat{y}_t^S \quad \forall t = N \dots N + m - 1$ 
11 Return  $\{y_t\}_{t=N}^{N+m-1}$ 

```

pressure” numerical weather prediction (NWP) attributes. The incremental of these attributes is related to the change of the load. Hence, we do the difference operator to the NWP attributes 2 days before(always 192 points ahead).

RollingStatsFeaturizer is used for rolling history load data with different windows, such 1 or 7. Rolling history load represents the past loads influences to the future. It is essential for algorithm to learn historical patterns of load.

FeatureEnsembler is used for ensembling temporal, weather and load features together and then over-all features being inputs can drive model to predict future load.

Pred_one_component is used for predicting long-term trend, short-term trend,period components with different parameters. When to forecast long-term trend the parameter *model* = 'linear'. In the case of predicting short-term trend the parameter *model* = 'evloss'. For forecasting period, the parameter *model* = 'lgb'. The final predicted value is the

Algorithm 2: Framework Experiments Procedure

- 1 DateTimeFeaturizer
- 2 DifferenceFeaturizer
- 3 RollingStatsFeaturizer
- 4 FeatureEnsembler
- 5 Pred_one_component

sum of above components.

F. EXPERIMENTAL RESULTS

F.1. Visualization of the Predicted Curve

In Figure 9 we show the curve predicted by SaDI and baselines. Four sub-cases (Hubei, Hunan, Jiangxi, and Henan) in the dataset of Huazhong are illustrated. We select a window of 7-day extreme event. The Y axis is masked for confidentiality purposes.

As shown in Figure 9, we visualize the curve predicted by models during extreme events. It is easy to observe that canonical LightGBM model failed to capture the temporal growth of load due to difficulty in extrapolation for tree-based model as we mentioned above, especially for the unseen peak in history. Introducing EVL into LightGBM makes the prediction better, but the gap between the prediction and the ground truth is still remarkable. LDS has comparable performance with SaDI, however, being a TCN-based model, its computational cost is much higher.

F.2. Comparison of ‘Success Rate’

Define $\mathbf{y} = [y_0, \dots, y_{m-1}]$, $\mathbf{x}_t^h = [x_{t,0}^h, \dots, x_{t,p-1}^h]$, $\mathbf{x}_t^e = [x_{t,0}^e, \dots, x_{t,q-1}^e]$, and $\mathbf{x}_t = [(\mathbf{x}_t^h)^T, (\mathbf{x}_t^e)^T]^T$. Here, we aim to find a function $f(\cdot)$ such that the success rate of prediction is maximized. A prediction is said to be successful if the normalized root mean square error (nRMSE) is less than a predefined threshold η . We denote the success rate with threshold η as SR@ η . Then, given a set of $\{(\mathbf{x}_t, y_t)\}$, we aim

Table 5: Ablation study of SaDI on pulic dataset.

| Datasets | Peacock | | Rat | | Robin | |
|--------------------------|--------------------|-------------------|--------------------|-------------------|--------------------|-------------------|
| Metrics | nRMSE _d | MAPE _d | nRMSE _d | MAPE _d | nRMSE _d | MAPE _d |
| SaDI | 0.0250 | 0.0208 | 0.0855 | 0.0772 | 0.0682 | 0.0599 |
| SaDI wo decompose | 0.0579 | 0.0464 | 0.1628 | 0.1515 | 0.1151 | 0.1014 |
| SaDI wo Feature engineer | 0.2192 | 0.2088 | 0.3181 | 0.2900 | 0.1566 | 0.1353 |
| SaDI wo EVL | 0.0254 | 0.0212 | 0.0914 | 0.0835 | 0.0691 | 0.0609 |
| SaDI w GAM | 0.0284 | 0.0234 | 0.0901 | 0.0798 | 0.0737 | 0.0642 |

to maximize:

$$SR@η = \mathbb{E} \left[\mathcal{I} \left(\sqrt{\frac{1}{m} \sum_{t=0}^{m-1} \frac{(y_t - f(\mathbf{x}_t))^2}{y_t^2}} \leq \eta \right) \right] \quad (8)$$

where $\mathcal{I}(Q)$ is an indicator function that equals to 1 if Q is true and 0 otherwise. We note that directly optimizing $SR@η$ is difficult due to its non-differential property. To address this issue, in the following section, we propose a decomposition-based model. Moreover, in order to enhance robustness against extreme events, we introduce a self-adaptive loss that can adaptively assign weights according to the fitting error of each time stamp.

In Figure 8, we plot the success rate defined in Equation 8 with various thresholds $η \in [0.8, 1]$. It is observed that the success rate of SaDI outperforms all other baselines with a range of different $η$.

F.3. Ablation Study

Table 5 shows that the ablation of any module will degrade the performance. It is worth noting that we implement GAM using GBDT with a depth of 1. GAM has worse performance than deeper boosting tree model. Thus, SaDI with GAM sacrifices the performance to gain interpretability.

F.4. Evaluation of Speed

Table 6: Comparison of SaDI and baselines on training speed and inference speed.

| Methods | SaDI | LightGBM | EVT | LDS |
|--------------------|-------------|----------|-------------|-------|
| Training time (s) | 71.8 | 88.7 | 225.7 | 110.2 |
| Inference time (s) | 0.972 | 0.695 | 0.07 | 1.51 |

As shown in Table 6, SaDI has the shortest training speed among all baselines. The integrated GAM in SaDI is light-weighted. SaDI has a higher inference time since the three decomposed issues will be predicted individually and then summed up. However, the long inference time is acceptable.

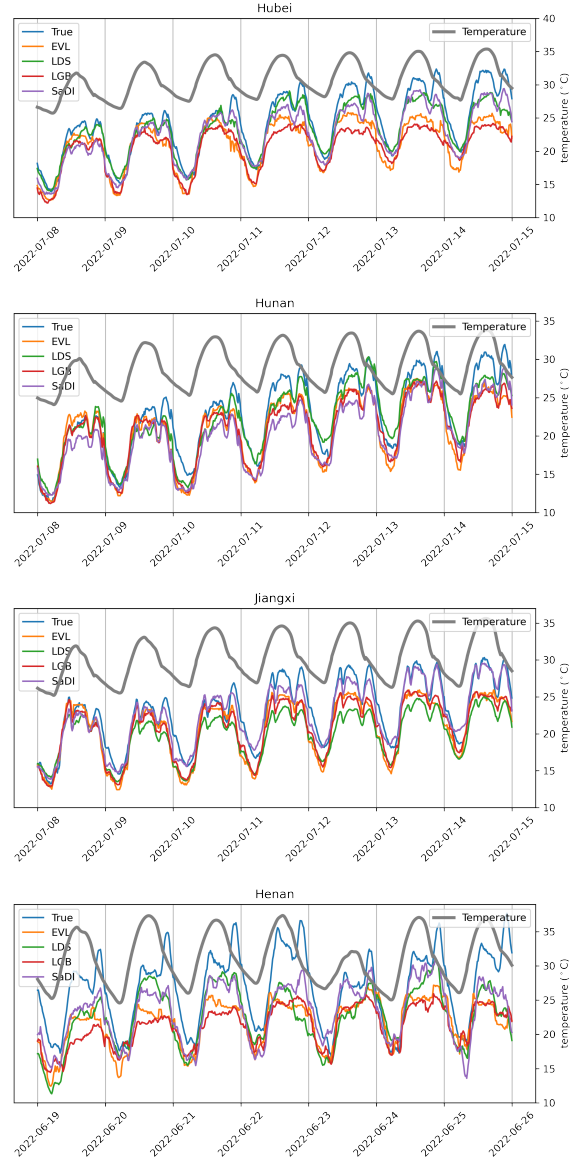


Fig. 9: Performance comparison of SaDI with canonical LightGBM model and two baselines (EVT and LDS) designed for dealing with extreme events. We select two 7-day extreme events on the datasets of Hubei (up) and Hunan (down). The Y axis is masked for confidentiality purposes.